A Femtosecond Pulse-Shaping Apparatus Containing Microlens Arrays for Use with Pixellated Spatial Light Modulators

Keith M. Mahoney and Andrew M. Weiner, *Fellow, IEEE*

Abstract— **We discuss a modified femtosecond pulse shaper that uses microlens arrays to convert the continuous band of frequencies normally obtained at the mask plane of a pulse shaper to a series of discrete spots. Two possible modified pulse-shaping geometries are described and the optimum geometry is chosen. Our experiments demonstrate that this modification can improve pulse-shaping quality when modulator arrays with large interpixel gaps are used for Fourier-plane filtering.**

I. Introduction

FEMTOSECOND pulse shapers have been used to produce tailor-made pulse shapes for use in many applications such as high-speed communications, nonlinear fiber optics, and ultrafast spectroscopy [1]. Pulse shaping has been demonstrated using fixed amplitude or phase masks [2], holograms [3]–[5], and moving mirrors [6] to spatially filter the frequency components in the zero-dispersion pulse compressor. Programmable pulse shapes can be produced by replacing the above spatial filters with a liquid-crystal modulator array [7]–[9]. This allows the pulse shapes to be modified on a millisecond time scale with gray level control by adjusting the pixels in the modulator array corresponding to the amplitude or phase of the individual frequency components. The programmability adds flexibility to the pulse-shaping setup, but needs to be updated at a faster rate for use in future high-speed communication systems. Pulse shapers have been designed which use acoustooptic modulators to perform the spatial filtering [10] and can be modified on a microsecond time scale for low-repetition-rate applications (e.g., femtosecond pulse amplifier systems). Optoelectronic device arrays, based on SEED [11] or other multiple-quantum-well (MQW) technologies, e.g., [12], offer the potential for pulse shaping with subnanosecond reprogramming times. But the optoelectronic device arrays are typically fabricated in such a way that the active pixels that modulate the light are small and are separated by inactive regions between the pixels. One example of this are MQW-SEED arrays, which have been used inside of a pulse shaper to carve a femtosecond pulse into a number of separate wavelength channels for wavelength division multiplexed (WDM) optical communications [13]. The MQW-SEED arrays are an attractive technology for modulator arrays because of their rapid reprogrammablility (>100 Mb/s); however, in order to achieve high speed, these arrays must have small device cross-sectional areas leading to low fill factors (~25% for the arrays used in [13]) and large gaps. For time-domain pulse-shaping applications, this is a problem because the discrete pixels cannot efficiently modulate the continuous band of frequencies that are present in the pulse shaper.

In this paper, we propose and demonstrate a way to avoid this mismatch between the conventional pulse shaper and the high-speed modulator arrays by adding microlens arrays inside the pulse shaper [14]. The continuous line of light (corresponding to the spatially dispersed optical frequencies in the input pulse) is focused to a one-dimensional array of spots by the individual microlenses in the array. Since the light is focused to discrete spots rather than spread out in a continuous band, a pixellated modulator array can be used at the masking plane to perform the pulse-shaping spatial filtering. We discuss experimental results which show that our modified pulse shaper can be used to achieve high-quality pulse shaping even for low-fill-factor modulator arrays, although the effects of the interpixel gaps cannot be eliminated entirely.

The format of this paper is as follows. Section II describes the conventional pulse shaper and reviews the basis of pulse shaping. Two modified pulse geometries using microlens arrays are introduced in Section III. An experimental demonstration of improved pulse shaping with pixellated masks is presented in Section IV. We conclude in Section V.

II. Conventional Pulse Shaper

One method for producing shaped femtosecond pulses involves using a zero-dispersion pulse compressor to spectrally filter the optical pulse [1], [2]. This is accomplished by a pulse-shaping apparatus that consists of a pair of lenses and gratings. The two lenses are spaced apart at twice the focal length and the gratings are placed one focal length from the lenses as shown in Fig. 1. An ultrashort light pulse is input to the grating on the left which angularly disperses the frequency components that comprise the pulse. The different frequency components are spatially dispersed and focused at the mask plane (halfway between the two lenses), so that the frequencies form a continuous one-dimensional line that directly corresponds to the spectrum of the pulse. The beams

Manuscript received April 17, 1996. This work was supported in part by the National Science Foundation under Grant ECS-9 312 256 and by the Air Force Office of Scientific Research under Contract F49620–95–1–0533.

The authors are with the School of Electrical and Computer Engineering, Purdue University, West Lafayette, IN 47907-1285 USA.

Publisher Item Identifier S 0018-9197(96)08656-3.

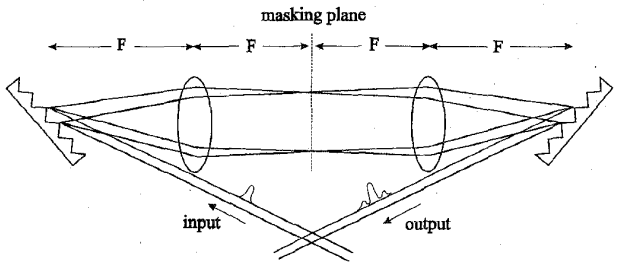

Fig. 1. Schematic of the conventional pulse shaper. The optical components are arranged in a $4F$ system with F being the bulk lens focal length.

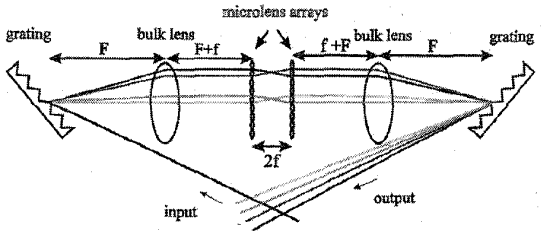

Fig. 2. One proposed modified pulse-shaping geometry where two microlens arrays are placed in the middle of the pulse shaper. The focal length of the bulk lens and microlens are denoted by F and f, respectively.

then propagate through the second lens which recombines them into a single spot on the output grating. The beams diffract off the second grating to produce a single output beam. The setup as described is dispersion-free, meaning that all of the frequency components travel the same optical path length through the pulse shaper. If no filter is placed at the masking plane, the output pulse is exactly the same as the input. The output pulse can be shaped by placing a spatially patterned amplitude or phase filter at the masking plane to modify the frequency spectrum. The output pulse shape is determined by the Fourier transform of the pattern transferred by the mask onto the spectrum. A broad range of optical waveforms can be generated by determining the appropriate frequency filter and applying it to the optical frequencies with a spatial mask.

III. A Modified Pulse Shaper

In addition to spatially dispersing the optical frequency components at an internal masking plane, a pulse-shaping system must be dispersion-free and must recombine all of the frequency components so that they produce a single collimated output beam. In order to determine a modified pulse-shaping geometry that uses microlens and which meets these requirements, we performed a ray-tracing analysis to model the optical system. Conventional ray-tracing cannot be used because the pulse shaper contains dispersive elements, such as diffraction gratings, that cannot be modeled by ABCD matrices. There are a variety of methods developed to model optical systems containing dispersive elements [15]–[17]. The method that we chose uses 4×4 matrices (as compared to the 2×2 in conventional ray-tracing) to describe the properties of the optical components [15]. Using these techniques, the entire pulse-shaping setup, from input grating to output grating, can be characterized as a product of the 4×4 matrices using our algorithm. The position of the optical rays are calculated for a global position, which was defined relative to the bulk lens, for the input grating and first bulk lens. When the rays encounter the microlenses arrays, the algorithm converts the position from a global position to a series of local positions, which relates the position of the optical rays to each individual microlens. The optical rays are calculated using the local position until they exit the last microlens array and then are converted back to a global position for the last bulk lens and the grating. We considered two pulse-shaping geometries involving microlens arrays. The first used a pair of microlens arrays placed into the center of the conventional pulse shaper as shown in Fig. 2. This geometry generated a series of discrete spots that can be used with pixellated modulator arrays and had zero dispersion, but it did not generate a single collimated output beam. Therefore, we designed a second geometry using two pairs of microlens arrays that still satisfies the above two conditions and does produce a single collimated output beam. We will first describe the design and the experimental results with the two microlens array geometry that fails to produce a collimated beam in order to gain insight into the characteristics of the pulse shapers using microlens arrays. Then we will describe the correct, four-microlens array geometry.

For the geometry shown in Fig. 2, the bulk lens is placed one focal length away from the grating, the distance between the microlens array and the bulk lens is the sum of the bulk lens and microlens focal length, and the microlens arrays are separated by twice the microlens focal length. When using the geometry in Fig. 2, the first microlens array converts the continuous line of focused frequencies into a one-dimensional array of discrete spots that corresponds to the active regions of the modulator array. The second microlens array then images the discrete spots back into a continuous band of frequencies. The arrangement of microlens arrays does provide the discrete line of spots required for the pixellated modulator array, but it is not the geometry that can be used to produce shaped pulses. The reason for this is that the two microlens arrays act like an array of telescopes that mix up the locations of the optical frequencies. This causes the frequency components that lie on a single microlens to be arranged in a reverse order after the second microlens. When these frequencies are focused onto the output grating, the input angle for a specific frequency is different than the angle with which it diffracted off of the first grating. This causes the second grating to diffract the different frequencies at different output angles. As a result, the output beam observed at some distance away from the second grating has an elliptical shape instead of circular. One experimental measurement of the frequency variation along the long axis of the elliptical output beam is shown in Fig. 3. We used gratings with 1800 lines/mm, a bulk lens with focal length of 150 mm, and microlens arrays fabricated by United Technologies Adaptive Optics Associates (AOA-0100-1.7-S) that are arranged in a two-dimension 6.8 $\times$ 6.8 mm square array that have a center-to-center spacing of 100 μm, >98% fill factor, and a focal length of 1.7 mm. For our work, we only used one row of each two-dimensional array. Fig. 3(a) is the spectrum measured on one end of the elliptical beam and

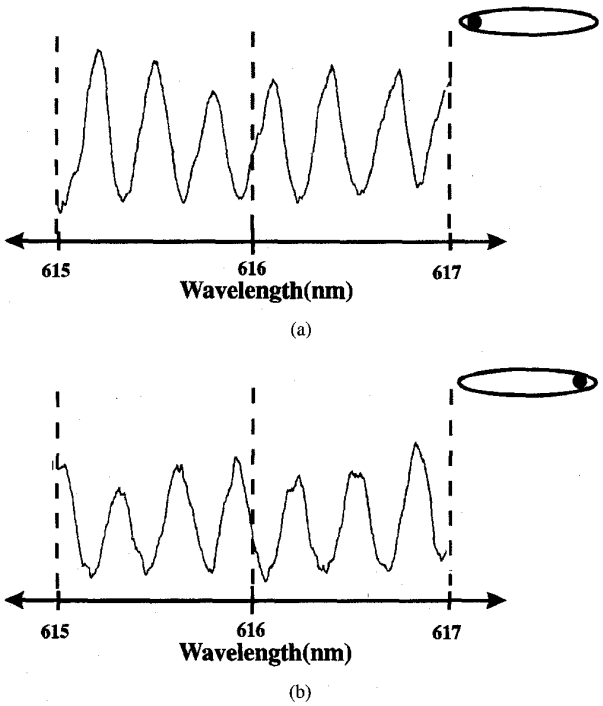

Fig. 3. Spectral measurements taken from two locations of the elliptical output beam generated by the modified pulse shaper in Fig. 2.

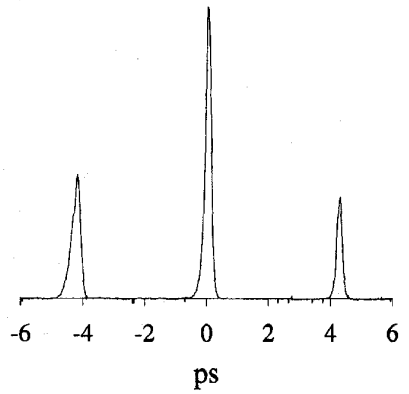

Fig. 4. Cross correlation showing the temporal profile generated by the modified pulse shaper in Fig. 2.

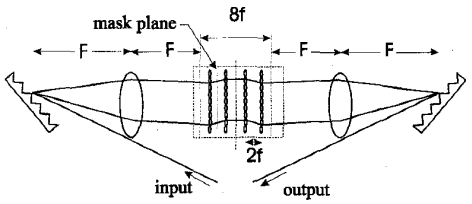

Fig. 5. Another modified pulse-shaping geometry that uses four microlens arrays. The microlens arrays are separated by twice the microlens focal length (f) and the grating to bulk lens spacing is the bulk lens focal length (F).

Fig. 3(b) shows the spectrum on the opposite end of the beam. A deep periodic modulation is observed and the modulation corresponding to the two ends of the elliptic beam are out of phase with each other. These features arise because of the periodic nature of the microlens array. At the mask plane, 1 mm spatially represents 3.03 nm of optical bandwidth, based on the equation

$$\Delta\lambda = \frac{d\cos\theta_d}{F}\Delta x$$

where $\Delta\lambda$ is the variation in wavelength, Δx is the spatial position, c is the speed of light, d is the grating period, $\theta_d = 35°$ is the diffraction angle off of the first grating, F is the focal length of the bulk lens, and λ is the wavelength. With a microlens center-to-center spacing of 100 μm, frequencies that are separated by 0.3 nm will have the same output diffraction angle. So at a spatial location corresponding to a certain output angle, the spectrum shows a modulation with 0.3-nm period.

An intensity cross-correlation measurement of the output shape generated by the modified pulse shaper that uses two microlens arrays is shown in Fig. 4 using an unshaped pulse from our CPM laser as a reference. The output pulse shape is a main peak along with two large sidelobes at ± 4.3 ps. The exact shape is sensitive to the position of the output beam that is sampled. The sidelobes are presumably caused by the deep modulation of the spectrum due to the angular errors as described above.

To correct these undesirable effects, the microlens arrays must be placed so that the frequencies are in the correct order before the light is focused onto the output grating. That will ensure that all the frequency components that diffract off of the second grating will have the same output angle. A second geometry was considered that allowed the frequencies to be focused to discrete spots and still maintain the correct order. Fig. 5 shows the geometry that we have designed using Kostenbauder's matrices. Our modified pulse shaper is similar to the conventional pulse shaper with the addition of four microlens arrays between the two bulk lenses. The bulk lenses are placed one focal length from the gratings. The four microlens arrays are spaced so that they form a pair of telescopes. The first and the second microlens array (as are the third and fourth array) are separated by twice the microlens focal length. The first microlens array converts the continuous band of frequencies into a one-dimensional array of spots that are centered at the middle of each microlens. The second microlens array changes the discrete spots back to a continuous line of mixed-up frequencies. The third and fourth microlens arrays form the second telescope which swaps the frequencies back and repositions them back to the correct order. The second bulk lens focuses the frequencies down onto the output grating. All of the frequencies are diffracted off of the second grating at the same position into the same direction and produce a collimated output beam. In this modified pulse shaper, the mask plane is between the first and second (or third and fourth) microlens array. As in the conventional pulse shaper, the shaped output pulse is determined by the Fourier transform of the filter pattern transferred by the mask onto the spectrum.

Figure 6 is an expanded view of the four microlens arrays in the center of the modified pulse shaper showing the ray-tracing calculations. For our calculations, we used parameters that model the commercial microlens arrays used in our

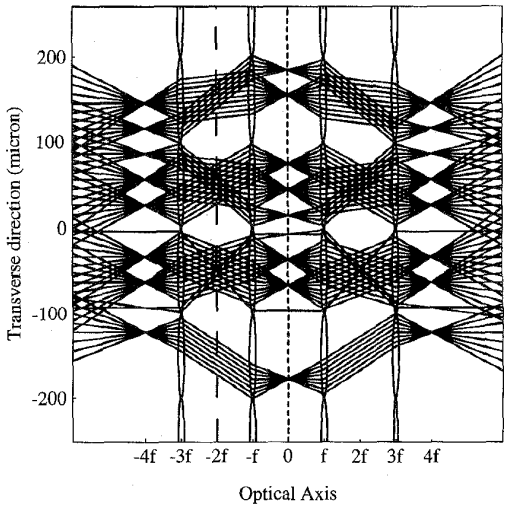

Fig. 6. A ray-tracing calculation showing the optical rays inside the modified pulse shaper as they pass through the four microlens arrays at distances of $-3f, -f, f$ and $3f$ as measured from position 0, the symmetry plane. The mask plane is located at $-2f$ between the first and second microlens arrays.

experiments. The diameter of each microlens is 100 μm with a focal length of 1.7 mm. The microlens arrays are spaced at distances described above. The series of focused spots to the left of the first microlens array represent individual frequency components focused by the first bulk lens. In the pulse shaper, each frequency is focused to a single spot at a different vertical position. Although the different focused spots actually form a continuous line, in the figure only a discrete set of frequencies are plotted. For a given frequency, the different rays represent different positions with the input spatial profile. The focal plane of the first bulk lens is one microlens focal length from the first microlens array. Light from different frequencies reaching an individual microlens is collimated toward the center of that microlens. Even the light that hits the edge of the microlens is directed toward an area at the center of the microlens. The second microlens array takes the light and focuses the frequencies back to a continuous band of frequencies at the symmetry plane. The right half of the figure is a mirror image of the left half and is used to orient the frequencies so that they exit the system in the same position as they entered.

By looking at the ray-tracing diagram, it can be seen that the microlens array directs the light to the center of each microlens between the first and second array. This is the discrete array of spots that is needed to mate the modified pulse shaper with a pixellated modulator array. Thus, this geometry satisfies the first of our design criteria. The 4×4 ray-pulse matrices also shows that this geometry remains dispersion-free, satisfying our second design requirement. The final requirement is that the frequencies must not be transposed, which would produce an irregularly shaped output beam, as was observed in the two-microlens-array geometry. By looking at Fig. 6, it can be seen that all of the frequencies on the right-hand side appear in the same order as they do on the left-hand side. This shows that the four-microlens-array geometry does not disturb the orientation of the frequencies.

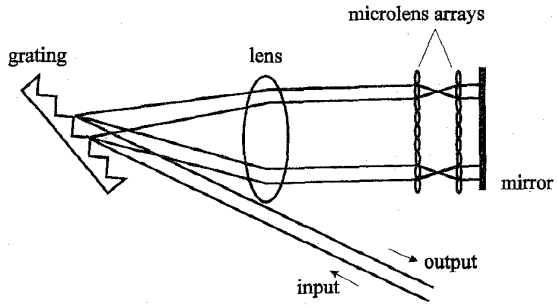

Fig. 7. A modified pulse-shaping geometry using a pair of microlens arrays in a reflection geometry. This setup is equivalent to the geometry shown in Fig. 5 using four microlens arrays in a single-pass geometry.

The ray-tracing analysis shown in Fig. 6 is an ideal treatment and does not model effects such as Gaussian beams, diffraction by the edges of the microlens, and imperfections in the shape of the lens. When these effects are taken into consideration, the actual field distribution will be somewhat modified. Firstly, the beams should be Gaussian, which means that the frequencies do not focus down to a point but instead down to a minimum beam waist. Secondly, frequencies that focus on the boundary between two microlens will experience enhanced diffraction and scattering. This will lead to dips in the spectrum caused by light hitting the edge of the microlens which represents a limit on the fidelity possible when shaping pulse with the modified pulse shaper.

IV. Experimental Results

When setting up the modified pulse shaper for our experiments, we decided to use a reflection geometry in which a mirror is placed at the plane of symmetry between the second and third microlens array as shown in Fig. 7. Using the reflection geometry allows the use of two microlens arrays instead of four, which simplifies the alignment procedure and reduces the number of components. The frequencies form discrete spots after the first microlens array, are converted to a continuous band after the second array, and are reflected by the mirror. The light is retroflected through the system and the output beam propagates in a direction opposite from the input beam. In our experiments, we used a CPM dye laser [18] that produced sub-100-fs pulses at a wavelength of 620 nm. The components used are the same 1800 lines/mm grating, a 150-mm focal length bulk lens, and microlens arrays with a 100-μm center-to-center spacing, >98% fill factor, and 1.7 mm focal length used in the previous experiment. As before, only a single row of each two-dimensional square microlens array was used for these experiments.

One characteristic of a pulse shaper that needs to be maintained is that it should not add any dispersion to the input optical waveform. We confirmed this is true for the modified pulse shaper by performing cross-correlation measurements on the output pulses obtained from the conventional and modified pulse shapers (without any spatial filters inserted at the masking plane). Fig. 8 shows that the cross-correlation data. The deconvolved pulses widths from the conventional and modified pulse shapers are 87 fs and 96 fs FWHM,

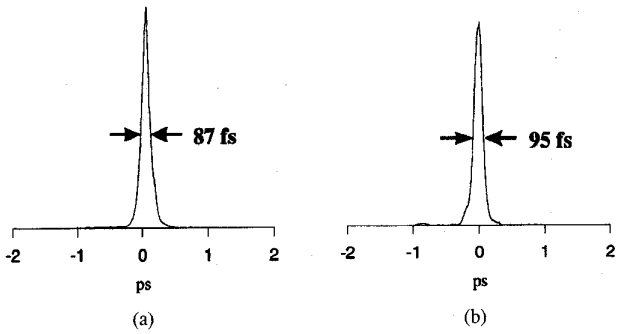

Fig. 8. Cross-correlation measurements of the output pulses from the conventional (a) and modified (b) pulse shapers with no mask present to perform the spatial filtering.

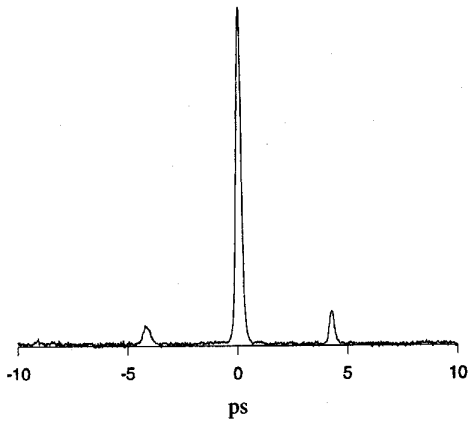

Fig. 9. Cross correlation of the output pulse from the modified pulse shaper with no mask present shown on a longer time scale to show the sidelobes at ±4.3 ps.

respectively, assuming a sech shape. The output pulse widths are comparable to the input pulse width; the difference between the conventional and modified case is within the day-to-day variation in pulse width from our CPM laser (these measurements were performed on different days). Therefore, we have shown that the modified pulse shaper is essentially dispersion-free. The output from the modified pulse shaper does have small satellite pulses at ±4.3 ps caused by light diffracted from the edges of individual microlenses as shown in Fig. 9. The microlens spacing of 100 μm corresponds to a series of dips in the spectrum with spacing $\Delta f = 2.37$ THz, which produces the sidelobes at ±4.3 ps. This effect is discussed in more detail later.

Now that the modified pulse-shaper geometry has been determined to be free of any added dispersion, the system needs to be tested by placing a pixellated modulator array at the mask plane of the modified pulse shaper. We fabricated a fixed amplitude mask that mimics a pixellated modulator as shown in Fig. 10. This was done by lithographically depositing metal on a substrate to form a series of masks that are each 1.5 mm wide, corresponding to each row, which will pass 4.54 nm of optical bandwidth (using the optical components previously listed). This is narrower than optical bandwidth of

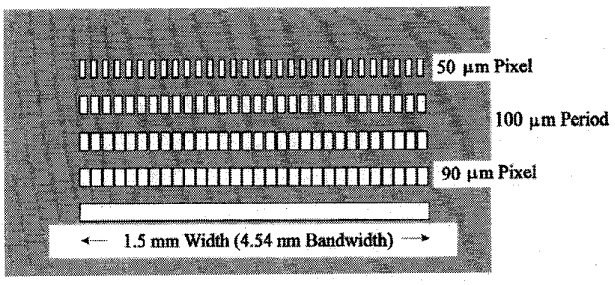

Fig. 10. Amplitude mask designed to mimic a modulator array with pixels on 100-μm centers. The five rows have 50-, 70-, 80-, 90-, and 100-μm active pixel widths, with 50-, 30-, 20-, 10-, and 0-μm dead space widths, respectively. The dead spaces correspond to opaque regions in the mask, while the active regions are transparent.

the CPM laser source and performs some simple pulse shaping by spectral windowing the input pulse to produce a broadened output pulse. Metal is deposited on regions that are designed to be opaque and clear regions are defined by areas without any metal deposition. Each mask is pixellated to imitate a modulator array. Each mask contains a series of clear areas that transmit light separated by opaque regions, corresponding to active pixels and deadspace, respectively. The pixels are spaced at 100 μm, which was designed to match the period of the microlenses in the array, and have a varying amount of active regions. Various filters are designed that have 100-, 90-, 80-, 70-, and 50-μm active regions. The 1.5-mm window is narrower than the width of the microlens array, so the light only passes through the 15 microlenses that are aligned with the corresponding pixels. The wide range of active regions allow us to design tests that will evaluate the effectiveness of the modified pulse shaper.

The amplitude filters were placed at the masking plane of the conventional and modified pulse shapers, and the resulting shaped output pulses were measured using standard SHG cross-correlation techniques using unshaped pulses directly from the CPM laser as a reference. The output pulses generated when placing the filter in the conventional and modified pulse shaper are shown in Fig. 11(a) and (b), respectively. Plots (i) represents the mask with 90-μm active region and 10 μm interpixel deadspace. Subsequent plots (ii), (iii), and (iv) are generated by the filters with 80/20 μm, 70/30 μm, and 50/50 μm active region/interpixel deadspace. When the filter is used inside the conventional pulse shaper, the intensity of the main pulse at $t = 0$ decreases dramatically as the interpixel deadspace increases, and heights of the sidelobes at ±4.3 ps increase relative to the central peak. This is caused by an increasing periodic spectral modulation due to frequencies striking the increasing interpixel deadspace. In contrast, for the modified pulse shaper, the intensities of the central peak and of the sidelobes stay roughly constant as the interpixel dead space is increased from 10 μm [Fig. 11(b): (i)] to 50 μm deadspace [Fig. 11(b): (iv)]. The sidelobe intensities are ~5–12% relative to the main peak at $t = 0$. This is approximately the same as the sidelobe height obtained with no pulse-shaping mask at the masking plane. This data clearly demonstrates that the microlens arrays are successful in circumventing the effect of interpixel deadspace.

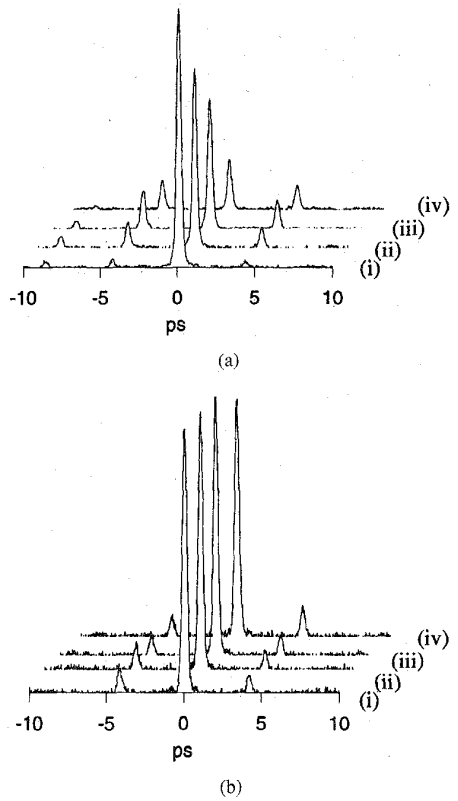

Fig. 11. Intensity cross-correlation measurements of the output pulses from the conventional (a) and modified (b) pulse shaper. The waveforms produced when using a mask that has 90-μm pixels with 10-μm gap (i), 80-μm pixel/20-μm gap mask (ii), 70-μm pixel/30-μm gap (iii), and 50-μm pixel/50-μm gap (iv) are shown.

The lowest sidelobes are present when the amplitude filter with the 90-μm pixels is used in the conventional pulse shaper. It is lower than the modified pulse shaper because the periodic microlens arrays used in the modified pulse shaper causes some diffraction for the frequencies impinging at the edges of individual microlenses. Those sidelobes in the 100/0 case for the modified pulse shaper represent a limit in the improvement in pulse shape that can accomplished for the modified pulse shaper. For the 80-μm pixels with 20-μm deadspace, the modified pulse shaper produces sidelobe heights lower than the conventional pulse shaper. Therefore, the modified pulse shaper produces pulse shapes comparable to those produced by a conventional pulse shaper with active pixels that are between 80 and 90 μm wide. One can therefore define the "active region" of the 100-μm microlens to be 85 μm out of 100 μm (despite the fact that the actual microlens fill factor is ~98%). The modified pulse shaper shows the greatest improvement over the conventional pulse shaper for the 50-μm pixels with 50-μm interpixel deadspace (iv). The sidelobe height from the modified pulse shaper with the mask that has 50-μm pixels is 5–12% of the main pulse as compared to the 40–50% relative height for the sidelobes generated by the conventional pulse shaper.

The 85-mm effective aperture of the individual microlenses size is not a fundamental limit but is dependent on the input spot size, bulk lens focal length, and microlens focal length. The size of the input beam may be adjusted to give the optimum mask plane spot size for a given modulator array and still produce a small enough spot size at the microlens array so that each frequency is contained inside one microlens. The limit for our modified pulse shaper is not the deadspace of the pixellated mask but instead is caused by the scattering due to the edge of the microlens. To some extent, one may reduce the spot size at the microlens array by varying the input spot size, etc., but at the same time one must ensure that the sizes of the discrete spots at the masking plane remain sufficiently small. For our parameters, we estimate that the modified pulse shaper should improve the pulse-shape quality for active regions that are as small as ~15 μm with interpixel deadspace of 85 μm, although we have only performed experiments with active regions down to 50 μm.

V. Conclusion

We have shown that the pulse-shaping quality with pixellated modulator arrays is improved when used with a modified pulse-shaping geometry incorporating microlens arrays. Our work with fixed amplitude masks can be extended to amplitude and/or phase electronically programmable modulator arrays. The microlens array used in our modified pulse shaper produces higher quality pulse shapes than the conventional pulse shaper for modulators that have interpixel deadspace greater than 15 μm for a 100-μm pixel spacing. Our modified pulse-shaper system should allow the use of optoelectronic modulator arrays with nanosecond or subnanosecond reprogramming times. This would allow the generation of highly structured ultrafast optical waveforms which could be modified at communication rates.

Acknowledgment

The authors would like to thank Adaptive Optics Associates for use of the microlens arrays.

References

[1] A. M. Weiner, "Femtosecond optical pulse shaping and processing," *Progress in Quantum Electron.*, vol. 19, pp. 1–237, 1995.
[2] A. M. Weiner, J. P. Heritage, and E. M. Kirschner, "High-resolution femtosecond pulse shaping," *J. Opt. Soc. Amer. B*, vol. 5, pp. 1563–1572, 1988.
[3] A. M. Weiner, D. E. Leaird, D. H. Reitze, and E. G. Paek, "Femtosecond spectral holography," *IEEE J. Quantum Electron.*, vol. 28, pp. 2251–2260, 1992.
[4] M. C. Nuss and R. L. Morrison, "Time-domain images," *Opt. Lett.*, vol. 20, pp. 740–742, 1995.
[5] K. Ema and F. Shimizu, "Optical pulse shaping using a Fourier-transformed hologram," *Jpn. J. Appl. Phys.*, vol. 29, pp. 631–633, 1990.
[6] K. F. Kwong, D. Yankelevich, K. C. Chu, J. P. Heritage, and A. Dienes, "400-Hz mechanical scanning optical delay line," *Opt. Lett.*, vol. 18, pp. 558–560, 1993.
[7] A. M. Weiner, D. E. Leaird, J. S. Patel, and J. R. Wullert, II, "Programmable shaping of femtosecond optical pulses by use of 128-element liquid crystal phase modulator," *IEEE J. Quantum Electron.*, vol. 28, pp. 908–920, 1992.
[8] M. C. Wefers and K. A. Nelson, "Programmable phase and amplitude femtosecond pulse shaping," *Opt. Lett.*, vol 18, pp. 2032–2034, 1993.
[9] ——, "Generation of high-fidelity programmable ultrafast optical waveforms," *Opt. Lett.*, vol. 20, pp. 1047–1049, 1995.

[10] C. W. Hillegas, J. X. Tull, D. Goswami, D. Strickland, and W. S. Warren, "Femtosecond laser pulse shaping by use of microsecond radio-frequency pulses," *Opt. Lett.*, vol. 19, pp. 737–739, 1994.
[11] D. A. B. Miller, "Quantum-well self-electro-optic effect devices," *Opt. Quantum Electron.*, vol. 29, pp. S61–S98, 1990.
[12] Y. H. Yan, R. J. Simes, and L. A. Coldren, "Analysis and design of surface-normal Fabry–Perot electrooptic modulators," *IEEE J. Quantum Electron.*, vol. 25, pp. 2272–2280, 1989.
[13] E. A. De Souza, M. C. Nuss, W. H. Knox, and D. A. B. Miller, "Wavelength-division multiplexing with femtosecond pulses," *Opt. Lett.*, vol. 20, pp. 1166–1168, 1995.
[14] K. M. Mahoney and A. M. Weiner, "Modified femtosecond pulse shaper using microlens array," *Opt. Lett.*, vol. 21, pp. 812–814, 1996.
[15] A. G. Kostenbauder, "Ray-pulse matrices: A rational treatment for dispersive optical systems," *IEEE J. Quantum Electron.*, vol. 26, pp. 1148–1157, 1990.
[16] O. E. Martinez, "Matrix formalism for pulse compressors," *IEEE J. Quantum Electron.*, vol. 24, pp. 2530–2536, 1988.
[17] S. P. Dijaili, A. Dienes, and J. S. Smith, "ABCD matrices for dispersive pulse propagation," *IEEE J. Quantum Electron.*, vol. 26, pp. 1158–1164, 1990.
[18] J. A. Valdmanis, R. L. Fork, and J. P. Gordon, "Generation of optical pulses as short as 27 femtoseconds directly from a laser balancing self-phase modulation, group-velocity dispersion, saturable absorption, and saturable gain," *Opt. Lett.*, vol. 10, pp. 131–133, 1985.

Keith M. Mahoney was born in Cleveland, OH, on August 18, 1970. He received the B.S. degree in electrical engineering from Ohio University, Athens, and the M.S. degree in electrical engineering from Purdue University, West Lafayette, IN, in 1992 and 1994, respectively.

He joined Hewlett-Packard, Greeley, CO, in 1996 in the R&D area of the Greeley Hard Copy Division. In his current position, he is responsible for the design of optical scanning devices.

Mr. Mahoney is a member of the Optical Society of America.

Andrew M. Weiner (S'84–M'84–SM'91–F'95) was born in Boston, MA, in 1958. He received the Sc.D. degree in electrical engineering from the Massachusetts Institute of Technology (MIT), Cambridge, in 1984.

From 1979 to 1984, he was a Fannie and John Hertz Foundation Graduate Fellow at MIT. His doctoral thesis dealt with femtosecond pulse compression femtosecond dephasing in condensed matter. In 1984, he joined Bellcore where he conducted research on ultrafast optics, including shaping of ultrashort pulses, onlinear optics and switching in fibers, and spectral holography. In 1989, he became Manager of the Ultrafast Optics and Optical Signal Processing Research District. He assumed his current position of Professor of Electrical and Computer Engineering at Purdue University, West Lafayette, IN, in October 1992. His current research interests center on holography of ultrashort pulses, high-speed optical communcations, and applications of pulse shaping to femtosecond spectroscopy and nonlinear optics. He is currently a member of the IEEE LEOS Board of Governors and a Topical Editor of *Optics Letters*. He previously served as Associate Editor of IEEE JOURNAL OF QUANTUM ELECTRONICS and IEEE PHOTONICS TECHNOLOGY LETTERS. He has authored nearly 160 conference and university talks and nearly 80 technical articles, including four book chapters, and holds five US patents.

Prof. Weiner is a Fellow of the Optical Society of America (OSA). He was awarded the 1984 Hertz Foundation Doctoral Thesis Prize for his doctoral thesis. He has served as vice-chairman of the Gordon Conference on Nonlinear Optics and Lasers, chair of the ULtrafast Phenomena Technical Group of the OSA, chair of the OSA Adolph Lomb Medal Committee, member of the IEEE Education Medal Committee, and member of numerous conference committees. He was Program Co-Chair for the 1996 Conference on Lasers and Electro-optics. In 1988–1989, he served as IEEE LEOS Traveling Lecturer, and in 1990, he was awarded the Adolph Lomb Medal of the OSA for noteworthy contributions to optics made before reaching the age of 30.